Journal of *Marine Science and Engineering*

MDPI

Article

Assessing the Impact of Soil Hydrocarbon Properties on Plant Functional Types Using Hyperspectral Data in the Niger Delta

Abdullahi A. Kuta [1,2,*], Stephen Grebby [3], Doreen S. Boyd [4] and Christopher H. Vane [5]

[1] Nottingham Geospatial Institute, University of Nottingham, Nottingham NG7 2TU, UK
[2] Department of Civil Engineering, Nottingham Trent University, Nottingham NG1 5JS, UK
[3] UK Terra Motion Limited, Ingenuity Centre, Triumph Road, Nottingham NG7 2TU, UK; stephen.grebby@terramotion.co.uk
[4] School of Geography, University of Nottingham, Nottingham NG7 2RD, UK; doreen.boyd@nottingham.ac.uk
[5] British Geological Survey, Organic Geochemistry Facility, Keyworth, Nottingham NG12 5GG, UK; chv@bgs.ac.uk
* Correspondence: abdullahi.kuta@ntu.ac.uk or abdullahi_kuta@yahoo.com; Tel.: +44-74-7401-9838

Abstract

The presence of soil hydrocarbon parameters (SHPs), including total petroleum hydrocarbons (TPHs), total organic carbon (TOC; %), and soil toxicity (EC50; mg L^{-1}), can affect vegetation in several ways. This study assessed the impact of SHPs on vegetation in the Niger Delta using field-measured, leaf-scale hyperspectral data acquired across the region. Red-edge position (REP) and four hyperspectral vegetation indices (HVIs)—mND705, photochemical reflectance index (PRI), Normalised Difference Vegetation Vigour Index ($NDVVI_{844,447}$; a vegetation vigour index), and modified DATT (MDATT; a chlorophyll-sensitive red-edge index)—were used to quantify chlorophyll content in the vegetation types of Awolowo grass, elephant grass, mango trees, oil palm trees, and mangrove vegetation and to explore their variation with SHPs. The results show that mangrove vegetation was the most impacted by TPHs ($R = -0.683$), while mango vegetation was the most impacted by TOC ($R = -0.725$), based on Pearson correlation coefficients derived from the mND705 index. Similarly, mango and mangrove vegetation showed the strongest responses to soil toxicity (EC50; mg L^{-1}), based on Spearman correlation coefficients ($r_s = 0.657$ and $r_s = 0.870$, respectively) using the MDATT index. These findings highlight species-specific physiological responses to soil hydrocarbon contamination and demonstrate the applicability of red-edge-based hyperspectral techniques for assessing vegetation stress in complex coastal ecosystems such as the Niger Delta.

Keywords: chlorophyll content; hyperspectral vegetation indices; red-edge position; oil spill; hyperspectral remote sensing; field spectroscopy; soil toxicity; total petroleum hydrocarbon; total organic carbon

Academic Editors: Georgios Sylaios, Yang Song, Daniel Constantino Zacharias and Angelo Teixeira Lemos

Received: 24 March 2026
Revised: 28 April 2026
Accepted: 6 May 2026
Published: 12 May 2026

1. Introduction

For more than four decades, oil exploration and production activities have left a severely degraded environment in the Niger Delta region [1]. Extensive crude oil pipeline vandalism, attributed to activities by non-state actors in disputes over environmental management and regional development [2], has further exacerbated environmental damage, with vegetation being particularly affected. Over the decades, various plant species have suffered significant impacts from repeated oil spills into the soil. Consequently, there is

an urgent need to monitor vegetation health in the Niger Delta to optimally manage and ultimately restore the degraded ecosystem [3].

Hydrocarbon contamination of soils resulting from oil spills affects vegetation through multiple mechanisms. The effects include plant growth stress, reduction in chlorophyll content [4,5], and other biophysical and biochemical alterations in vegetation structure and function. Collectively, these changes lead to the modification of vegetation reflectance signatures [6], which are critical to the detection of soil hydrocarbons remotely via earth observation (EO). Effective EO requires field-based studies to ensure that EO assessments are defensible, reproducible, and relevant to local ecological conditions. In this context, field spectroscopy is particularly important, as it provides hyperspectral measurements of vegetation reflectance that determines the vegetation health and can ultimately be linked to EO platform-based [7].

Although many studies have examined vegetation physiological responses to environmental stress under controlled experimental conditions, relatively few have integrated remote sensing and field data under natural field conditions [8]. To the best of our knowledge, no studies in the Niger Delta have comprehensively examined the effects of soil hydrocarbon parameters (SHPs)—such as total petroleum hydrocarbons (TPHs)—alongside other soil properties, including total organic carbon (TOC%) and soil toxicity concentrations (EC50), on the health and spectral reflectance of different plant species. The only known study in Nigeria employing spectroscopy to assess oil spill impacts on vegetation was conducted by Omodanisi and Salami [9] in Lagos and Ogun States in southwestern Nigeria—regions that are ecologically distinct from the Niger Delta and did not focus on individual plant types. Remote sensing assessments of oil spill impacts on vegetation in the Niger Delta have largely focused on multispectral satellite imagery, vegetation indices (e.g., NDVI, SAVI, and EVI) [3,6,10,11] and land-cover classification to detect stress, degradation, or post-spill change at landscape scales [12–14]. While these approaches have improved the spatial detection of oil-impacted areas, they provide limited insight into plant-level physiological responses and inter-species variability. Although Adamu [15] demonstrated the spectral sensitivity of vegetation to oil-contaminated soils using multispectral indices, such responses have not been examined using field-based hyperspectral measurements at leaf scale. Consequently, this study is the first to assess how soil hydrocarbon parameters influence the spectral responses of different plant types by using in situ leaf-level hyperspectral data in the Niger Delta.

Evaluating individual plant species is essential because tolerance to hydrocarbon contamination varies significantly among species [16], and integrating EO allows these differential physiological responses to be quantified through species-specific variations in spectral reflectance. Therefore, this study investigates the impact of soil hydrocarbon parameters on dominant plant species in the Niger Delta, with the aim of determining species-specific physiological and spectral responses to soil hydrocarbon contamination that can ultimately be used to design an EO monitoring approach. Vegetation species in the Niger Delta exhibit species-specific physiological responses to soil hydrocarbon parameters (TPH, TOC, and EC50), which are consistently detectable through red-edge position and chlorophyll-sensitive hyperspectral indices.

2. Materials and Methods

2.1. Study Area

The study area is located in Rivers State, Niger Delta, Nigeria. Two sites were selected to represent contrasting geographical settings: Igwuruta, an upland environment (Figure 1(a1)), and Bodo, a shoreline environment (Figure 1(a2)). These two sites are approximately 53 km apart. Igwuruta is a semi-urban town (longitude 6°59′05″ E to 7°02′55″ E

and latitude 4°55′23″ N to 5°00′55″ N) in the Ikwerre Local Government Area of Rivers State, near the Omagwa community. It hosts Port Harcourt International Airport and lies a few kilometres from the city of Port Harcourt. The primary occupations of the inhabitants are trade, public and private employment in various government and private companies, and farming.

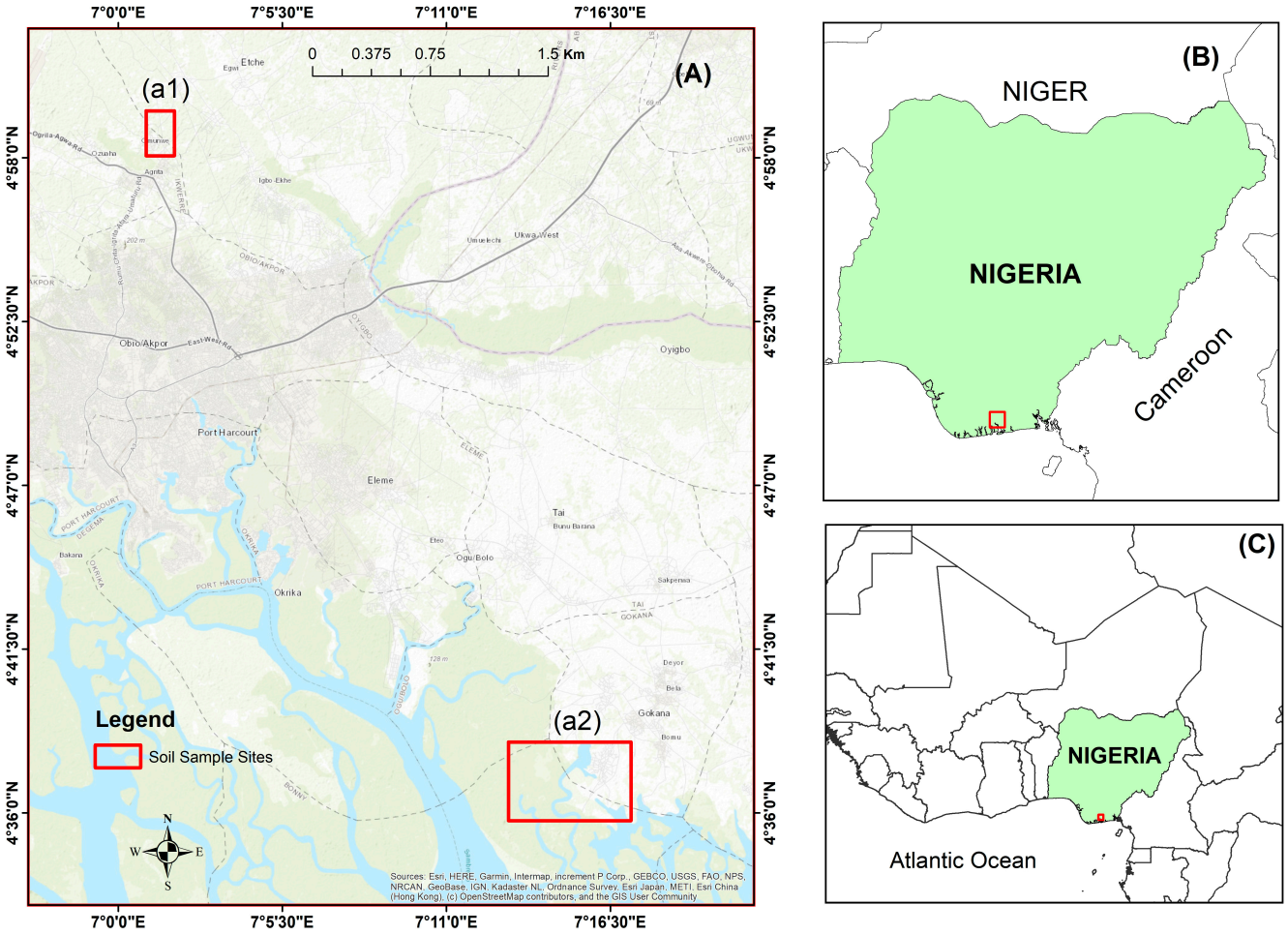

Figure 1. (**A**) Map of the study area showing the two sample sites (red box), (**B**) in relation to Nigeria and (**C**) in relation to West Africa. (**a1**) Upland sample location (soil sample points P1–P6) and (**a2**) shoreline sample location for dryland (P7–P13) and mangrove (P13–P22).

Bodo is a traditional rural and coastal Ogoni community with an estimated 69,000 inhabitants (longitude 7°13′45″ E to 7°17′38″ E and latitude 4°33′56″ N to 4°38′52″ N). It is administratively part of the Gokana Local Government Area of Rivers State, Nigeria [17]. The mangrove forests and waterways that line Bodo Creek are integral to the community's traditional livelihood system. Fishing and farming were the main occupations prior to extensive oil spill incidents, which severely disrupted these activities.

2.2. Plant Types

Across the two study areas, a range of dominant plant types exposed to repeated oil spill events were identified, including Awolowo grass, elephant grass, mango trees, oil palm trees, and mangrove vegetation (Figure 2).

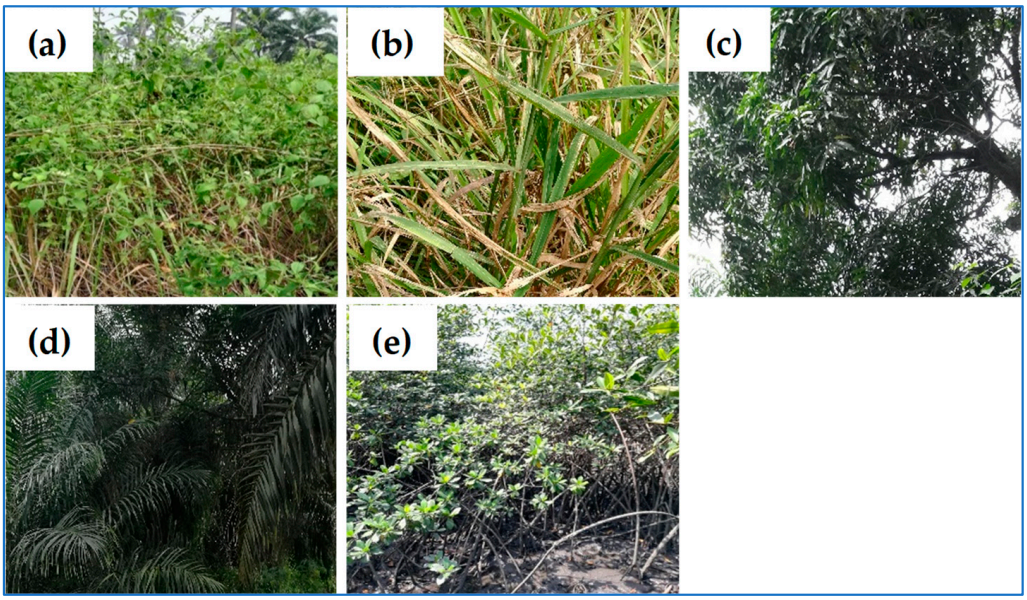

Figure 2. Leaf samples of (**a**) Awolowo grass, (**b**) elephant grass, (**c**) mango leaf, (**d**) oil palm leaf and (**e**) mangrove leaf obtained during field sampling.

2.2.1. Awolowo Grass

Chromolaena odorata (L.) R.M. King & H. Rob. (Asteraceae, Eupatorieae) is a perennial shrub that forms dense, tangled bushes approximately 1.5–2.0 m in height, occasionally reaching up to 6 m when scrambling over trees [18]. In Nigeria, it is commonly referred to as Awolowo weed, Akintola weed, or Queen Elizabeth weed and is native to the Americas, ranging from southern Florida to northern Argentina, including the Caribbean islands [19]. Awolowo weed is a widespread species found on wasteland, roadsides, and farmlands and occurs across most bushland in Nigeria [20]. Awolowo grass is often used as fallow vegetation because of its ability to act as a nutrient sink, its potential contribution to crops as a regular source of organic matter and nutrients after slashing, and its adaptability as a fallow plant on acidic soils when compared with some leguminous species [18].

2.2.2. Elephant Grass

Pennisetum purpureum, also known as elephant grass, Napier grass, or Uganda grass, is a tropical grass species native to humid tropical Africa and belongs to the family Poaceae [17]. Elephant grass is one of the fastest-growing plants globally and has long been an important forage crop in the tropics due to its high biomass yield and nutritional value [21]. There are two main types of elephant grass, giant (tall) and dwarf (short), with heights ranging from approximately 2 to 6 m.

2.2.3. Mango Tree

Mango (*Mangifera indica* L.) is an evergreen fruit crop indigenous to southern Asia, particularly eastern India, Burma, and the Andaman Islands. It is now one of the most widely cultivated and traded tropical and subtropical fruit crops globally [22]. The largest mango-producing countries include India, China, Thailand, Indonesia, Pakistan, Mexico, Brazil, Bangladesh, Nigeria, and the Philippines [23]. Mango trees typically reach heights of 15–30 m, although cultivated trees are often smaller, ranging from 3 to 10 m. In Nigeria, most mango trees are wild or semi-cultivated, and these were included in the present study [24].

2.2.4. Oil Palm Tree

Oil palm (*Elaeis guineensis* Jacq.) is the world's most productive oil-bearing crop and is naturally abundant in African rainforests [25]. It has the highest oil yield among cultivated oleaginous crops [16]. The species is indigenous to the Niger Delta and much of tropical Africa, and prior to 1900, the Niger Delta was a leading global exporter of palm oil and palm kernels [26]. Under natural conditions, oil palms can reach heights of 18–24 m, although cultivated palms typically remain between 6 and 9 m tall [27].

2.2.5. Mangrove Vegetation

Mangroves are woody shrubs or small trees that dominate the intertidal zones of tropical coastlines. In the Niger Delta, red mangroves (Rhizophoraceae) and white mangroves (Avicenniaceae) account for over 90% of mangrove vegetation, with *Rhizophora racemosa* being the dominant pioneer species [28]. This species play a critical socio-economic role for the coastal communities in Rivers State, providing resources for fuel, construction, and fishing activities [29].

2.3. Field Data Collection

During field data collection, the control (non-impacted) sites were not sampled due to a combination of security risks, restricted access, and ethical fieldwork considerations within the Niger Delta. Many areas that could potentially serve as reference sites were either inaccessible or had experienced undocumented or legacy hydrocarbon exposure, making it difficult to verify their suitability as true controls. To ensure researcher safety and data reliability, the study therefore focused on accessible oil-impacted sites and employed within-site and cross-vegetation comparisons as a robust alternative for assessing the effects of soil hydrocarbon parameters on vegetation health.

2.3.1. Leaf and Soil Sampling

Leaf and soil samples at oil spill sites in Bodo and Igwuruta were collected during the dry season (December 2018), when weather conditions were more favourable, with little to no rainfall [30]. Sample collection sites were selected based on accessibility, as random sampling was not feasible due to insecurity in the region. It is acknowledged that this sampling approach may introduce some unavoidable bias into the results. Leaf and soil samples were concurrently collected from each sampling plot. A total of 21 plots that have experienced oil spills along an oil pipeline corridor were sampled, covering the five vegetation types across the two land-cover types: dryland and mangrove. The dryland was further divided into shoreline and upland. This was done due to the availability of accessible sites and to determine if proximity to the shoreline could affect how hydrocarbons impact vegetation. Soil samples were collected to determine total petroleum hydrocarbons (TPHs) and other soil hydrocarbon parameters (SHPs) and to assess their effects on vegetation health [31,32]. Within each sample plot, five soil samples were collected at a depth of 30 cm—one from each corner and one from the centre—following established protocols [8]. Soil samples were collected at a depth of 30 cm to capture root-zone conditions and subsurface hydrocarbon accumulation, which are typical of oil-impacted soils in the Niger Delta. These subsamples were combined into a single composite sample representing each plot. All leaf and soil samples were stored in labelled, zip-locked plastic bags and placed in portable coolers during fieldwork [33]. Upon return from the field, soil samples were frozen to prevent exposure to temperatures exceeding 30 °C and to minimise further chemical reactions.

2.3.2. Leaf Spectral Measurements

Leaf spectral reflectance was measured using an ASD FieldSpec Pro (ASD, 2008), manufactured by Analytical Spectral Devices, Inc., Boulder, CO, USA, which is now a brand under Malvern Panalytical, following guidelines from the Field Spectroscopy Facility [34]. The instrument provides high-resolution hyperspectral measurements across the 350–2500 nm wavelength range. Measurements were conducted indoors under controlled laboratory conditions to minimise variability associated with ambient illumination.

A black enclosure lined with low-reflectivity material was constructed to prevent stray light interference. Reflective surfaces were covered with light-absorbent material to reduce noise and approximate darkroom conditions [35]. Two 100 W Lowel-Pro lamps provided consistent illumination. A white reference panel was used for instrument calibration, after which leaf samples were placed on a black background covering at least 90% of the field of view. Each spectral scan was averaged over 100 readings to improve the signal-to-noise ratio. For each leaf sample, 4–6 spectral measurements were collected at different positions and orientations to obtain representative reflectance spectra.

2.3.3. Postprocessing

Spectral data were processed using ViewSpec Pro software (ASD, 2008), which enables spectral visualisation, scaling, derivative analysis, and conversion into ASCII format [36]. Reflectance spectra and first derivatives were generated and exported for further analysis. For spectral shape analysis, reflectance signatures were averaged by plant type within each plot [37].

2.4. Soil Geochemistry Analysis

2.4.1. Solid-Phase Microbial Soil Toxicity (EC50 mg L^{-1})

Soil toxicity was assessed using the luminescent bacterium *Vibrio fischeri* (strain NRRL B-1117), which is highly sensitive to a wide range of chemicals and suitable for evaluating both acute and chronic soil toxicity. This methodology has previously been applied to soils and sediments from the UK and US [38–40]. Seven grams of dried soil were mixed with 35 mL of SPT diluent (3.5% NaCl) and stirred for 10 min to produce a representative suspension. A 1.5 mL aliquot was transferred to cooled SPT tubes, and a 1:2 serial dilution series was prepared, consisting of two controls and thirteen dilutions in duplicate. Freeze-dried *V. fischeri* was reconstituted with ultrapure water, and 20 µL of the bacterial reagent was added to each tube. Samples were incubated at 15 °C for 20 min and filtered to remove sediment, and 0.5 mL of the filtrate was transferred into cuvettes in a Microtox® M500 analyser, manufactured by Mirobics corporation, Alameda, CA, USA. Luminescence was measured after 5 min, and the resulting inhibition data were used to generate dose–response curves from which EC50 values were calculated to quantify soil toxicity.

2.4.2. Total Organic Carbon (TOC (%))

The total organic carbon content (TOC% wt/wt) was determined using an Elementar VarioMax C, N analyser manufactured by Elementar, Stockport, UK, operated in C mode. All soils were first prepared by acidification with HCl (50% v/v) to remove inorganic carbon (e.g., carbonate). The limits of quantification reported for a typical 300 mg sample were 0.18% (wt/wt) [41].

2.4.3. Total Petroleum Hydrocarbons (TPHs)

To measure the total petroleum hydrocarbon content (TPH), 1 g of ground sediment was extracted with a dichloromethane (DCM)/acetone (1:1 v/v) mixture by using an accelerated solvent extraction system (ASE 200, Dionex). Extracts were reduced to dryness and

reconstituted in 1 mL toluene, and 5 µL aliquots were spotted onto silica rods (Chromarods-S III). The rods were developed for 21 min using n-hexane, for 8 min with toluene and for 1.5 min with dichloromethane/methanol (9:1 v/v). The concentrations of saturated and aromatic hydrocarbons were determined using an Iatroscan Mk6 s instrument, manufactured by LSIM corporation, Japan [38,39]. The calibration was performed for saturated hydrocarbons using pristane, aromatic hydrocarbons using tripheylene, and resins using an in-house purified standard extracted from combined urban road-run-off sediments. TPH was calculated as the sum of saturated and aromatic hydrocarbons. The limit of quantification (LoQ) for total non-volatile petroleum hydrocarbons was 3 mg/kg.

2.5. Spectral Properties of Vegetation Calculation

2.5.1. First Derivative and Red-Edge Position (REP)

Derivative analysis was used to detect spectral absorption features, reduce spectral variations due to illumination and baseline shifts to reveal absorption features masked by broader interference from other leaf components and biochemical properties [37]. A common means of using spectral derivatives in the remote sensing of plant physiology has been to characterise the red edge [42]. The red edge is the point of maximum slope in vegetation reflectance spectra of 1st derivatives which occurs between the wavelengths of 680–750 nm. The red edge was used in this studies to determine the levels of change and stress related to plant chlorophyll content due to oil hydrocarbon properties. The red edge is a widely recognised spectral indicator of chlorophyll concentration, with its position and shape being strongly controlled by leaf pigment content [43,44].

2.5.2. Hyperspectral Vegetation Indices

The next analysis was the calculation of hyperspectral vegetation indices (HVIs). Many HVIs have been developed to estimate leaf pigment content [45]. Because the plant species assessed in this study exhibit notable differences in leaf surface structure, only indices that have previously demonstrated cross-species applicability—or have been successfully used in the study region—were selected. The HVIs with reflectance spectra in the Vis and NIR spectral ranges were considered because data in this part of the electromagnetic spectrum are informative in terms of leaf pigment variations [46]. The HVIs used for this study are summarised in Table 1.

Table 1. Summary of HVIs used for in this study.

Index	Equation		Source
mND705	(R750 − R705)/(R750 + R705 − 2R445)	Eq1	[45]
MDATT index	(R719 − R726)/(R719 − R743)	Eq2	[47]
$NDVVI_{844,447}$	(R844 − R447)/(R844 + R447)	Eq3	[8]
PRI	(R531 − R570)/(R531 + R570)	Eq4	[48]

R = the reflectance at a particular wavelength (in nm).

The mND705 spectral index is relatively insensitive to species and leaf structure variation, making it suitable for application in larger-scale remote sensing studies without extensive calibration. This is particularly relevant given that the present study considered plants with diverse leaf structures. The ND705 index, originally developed by Gitelson and Merzlyak [49], was modified by Sims and Gamon [45] to form the mND705 index using reflectance at 705 and 750 nm. This modification, based on the chlorophyll index, compensates for high leaf surface reflectance by incorporating reflectance at 445 nm, thereby reducing the effects of variations in leaf surface reflectance. This approach significantly improved correlations with chlorophyll content.

The MDATT index is a hyperspectral vegetation index developed by Lu et al. [47] to compensate for high leaf surface (specular) reflectance and mesophyll scattering. It is used for the remote estimation of chlorophyll content in plants with varying leaf surface structures, irrespective of leaf side or species composition. Among the reflectance indices tested by Lu et al. [47], the MDATT index performed the best among all the indices.

The Normalised Difference Vegetation Vigour Index (NDVVI) was developed by Onyia et al. [8] as a new method for monitoring the impact of oil pollution on vascular plants of various species observed in polluted and unpolluted (control) locations in the Niger Delta region using integrated satellite remote sensing and field data for biodiversity monitoring; it was used since it has proved effective in detecting the impact of hydrocarbon on vegetation in the Niger Delta.

The photochemical reflectance index (PRI), derived from narrowband reflectance at 531 and 570 nm wavelengths, was used to explore photosynthetic radiation use efficiency in 20 species representing three functional types, annual, deciduous perennial, and evergreen perennial, by Gamon et al. [48]. Although initially developed to estimate xanthophyll cycle pigment changes, it was related to carotenoid/chlorophyll ratios in green leaves [45].

2.6. Statistical Analysis

The association between the REP and SHPs, as well as plant types, was assessed based on statistical correlations (Spearman r_s and Pearson R) [50,51]. As the relationship between the SHPs (TPHs and soil parameters) and the spectral properties of leaf samples may not be linear, either Spearman and Pearson correlations were used.

3. Results

3.1. Soil Hydrocarbon Parameter (SHP) Concentrations

Table 2 summarises the soil sampling plot numbers, the corresponding plant types, and the measured soil parameters. Figures 3 and 4 present box plots and proportional symbol maps, respectively, illustrating the spatial distribution of total petroleum hydrocarbons (TPHs), soil toxicity (EC50), and total organic carbon (TOC, %) across six upland plots (P1–P6), seven shoreline dryland plots (P7–P13), and nine mangrove plots (P14–P22). The TPH concentration at plot P20 (24,996 mg kg^{-1}) was excluded from the mangrove box plot as an extreme outlier to avoid distortion of the distribution, and diamond symbols denote outlier values that differ substantially from the remaining observations. Soil toxicity levels were categorised as non-toxic (EC50 > 10,000 mg L^{-1}), moderately toxic (EC50 = 5000–10,000 mg L^{-1}), and highly toxic (EC50 < 5000 mg L^{-1}).

Table 2. Soil sample plot number, plant types sampled from each plot, and soil parameters.

Plot No.	Plant Types	Soil Toxicity (EC50 mg L^{-1})	Total Organic Carbon: TOC (%)	TPH mg kg^{-1} (Dry Weight Sediment)
P1	AG, EG, OP	27,899	1.58	642
P2	AG, EG	19,561	1.66	2247
P3	AG, EG, OP	27,309	1.86	1508
P4	AG, EG, OP	18,922	1.24	89
P5	AG, EG, OP	23,128	2.15	136
P6	AG, EG, OP	36,496	1.38	151
P7	AG, EG, MT, OP	40,423	0.8	212
P8	AG, EG, MT, OP	33,671	0.5	163
P9	AG, EG, OP	13,278	1.29	2606
P10	AG, EG, MT, OP	7986	1.27	770
P11	AG, EG, MT, OP	20,364	1.37	89
P12	AG, EG, MT, OP	37,792	0.96	89

Table 2. *Cont.*

Plot No.	Plant Types	Soil Toxicity (EC50 mg L^{-1})	Total Organic Carbon: TOC (%)	TPH mg kg^{-1} (Dry Weight Sediment)
P13	AG, EG, MT, OP	10,975	2.21	1174
P14	MG	4848	13.98	396
P15	MG	2525	26.17	89
P16	MG	3990	13.63	1887
P17	MG	2992	17.06	399
P18	MG	2672	15.74	393
P19	MG	19,168	1.97	996
P20	MG	14,248	13.85	42,996
P21	MG	29,720	0.61	329
P22	MG	6455	12.83	826
ADL		22,446	1.40	760
AM		9623	12.90	5368
TA		18,383	6.10	2645

Note: AG = Awolowo grass; EG = elephant grass; OP = oil palm; MT = mango tree; MG = mangrove; ADL = average values for dryland; AM = average alues for mangrove; TA = total average values for each soil property.

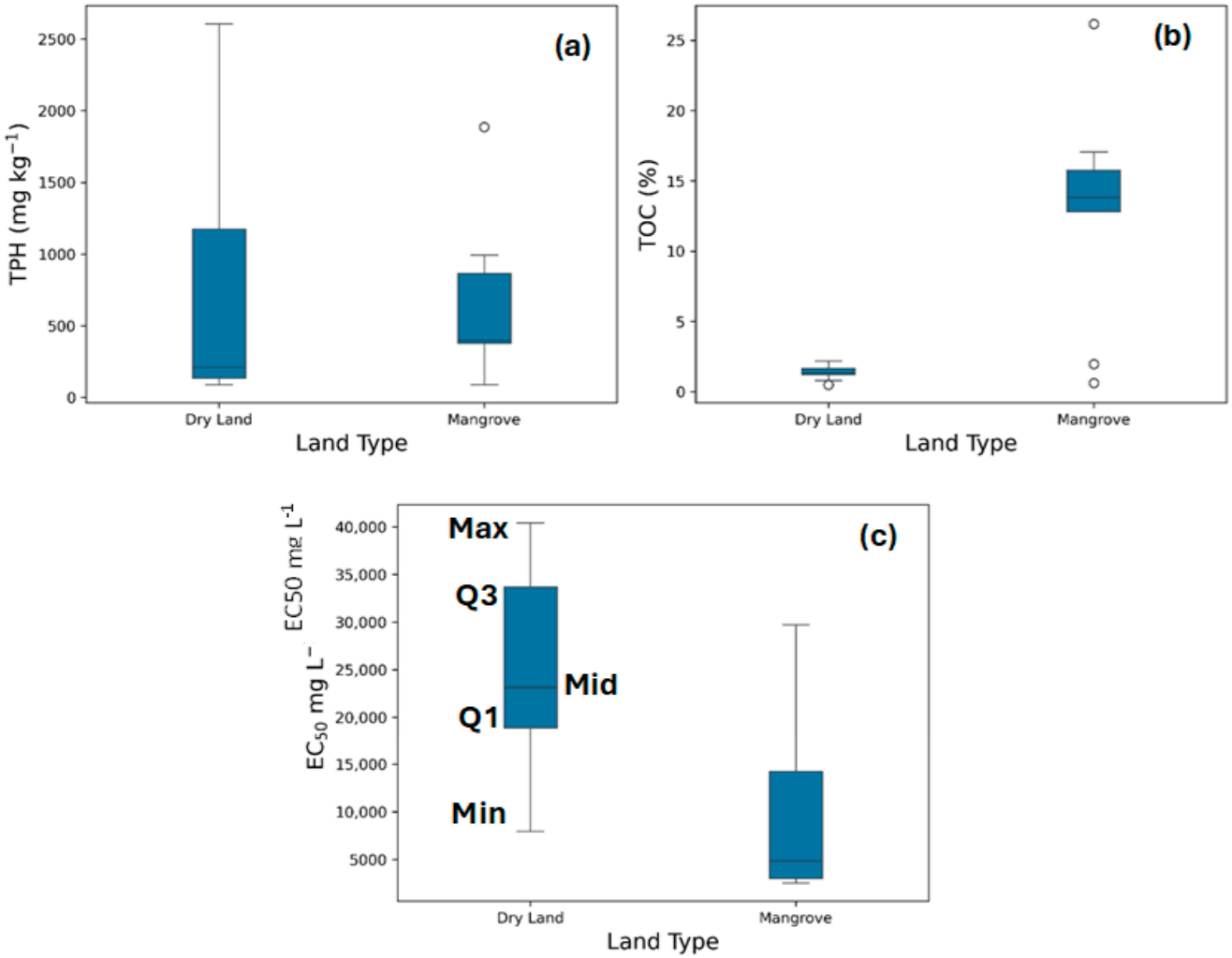

Figure 3. A box plot for (**a**) TPH (mg kg^{-1}), (**b**) toxicity (EC50 mg L^{-1}) and (**c**) TOC (%). Min and Max are the lowest and maximum values of the data, excluding the outliers. Q1 is the first quartile, at which the first 25% of the data falls. Q3 is the third quartile, the 75th percentile, while the Med is the median value that shows 50% of the data.

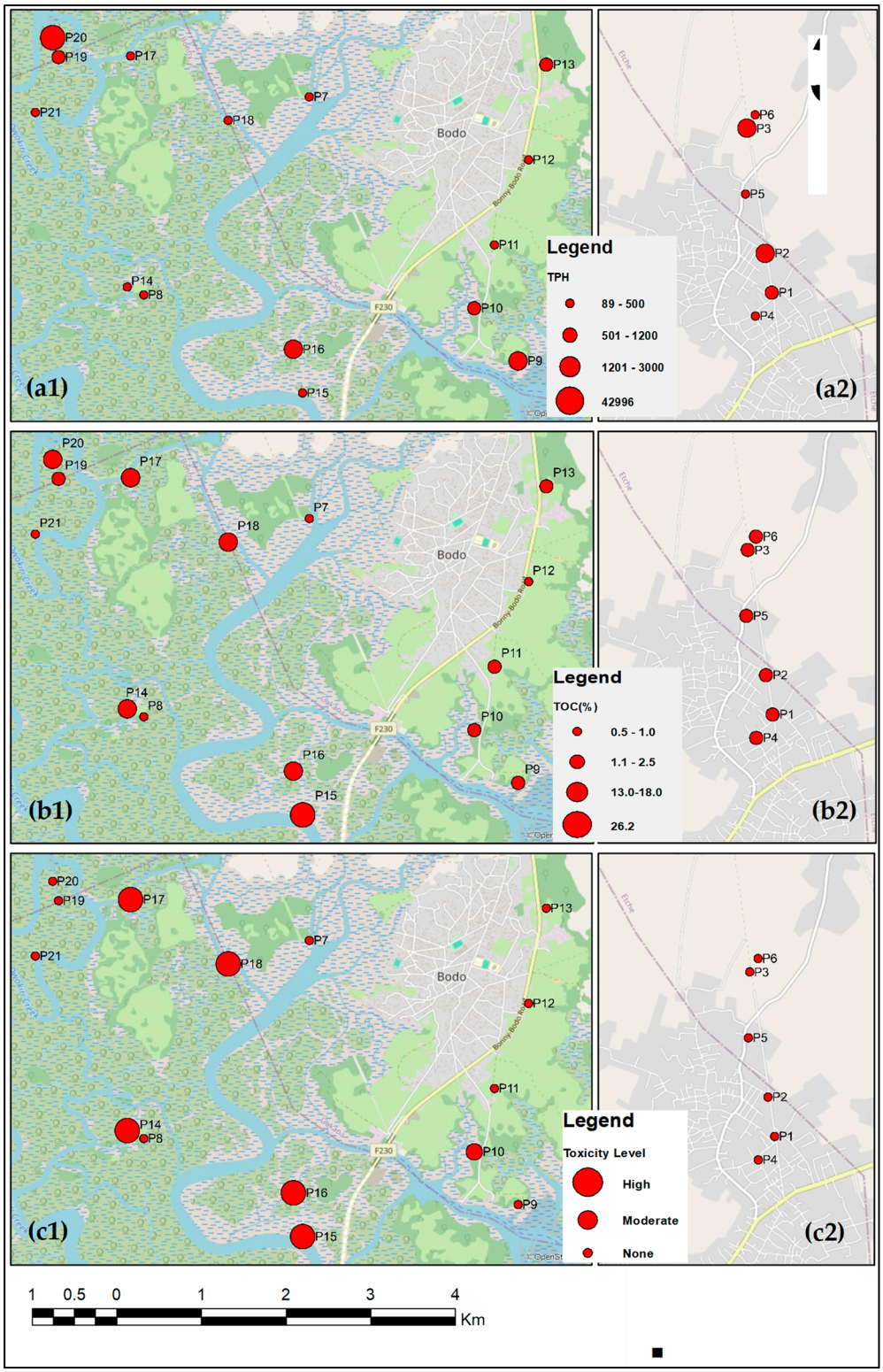

Figure 4. Soil hydrocarbon parameter content maps for shoreline/mangrove and upland (**a1**,**a2**) TPHs, (**b1**,**b2**) TOC (%) and (**c1**,**c2**) soil toxicity (EC50 mg L^{-1}).

The results indicate substantial spatial variability in SHP concentrations across land-cover types (Figure 3). For the TPH concentration, both dryland and mangrove environments had relatively the same level of concentration, except plot P20 in the mangrove zone (Table 2; Figure 4(a1)). However, the TOC concentrations were markedly higher in mangrove soils than in dryland soils (Figures 3b and 4(b1,b2)). Regarding soil toxicity, the patterns further distinguish mangrove from dryland environments. As shown in Figure 3c,

five of the nine mangrove plots (P14–P18) exhibited high toxicity (EC50 < 5000 mg L^{-1}), one plot showed moderate toxicity (P22), and three plots were non-toxic (P19–P21). In contrast, all upland plots (P1–P6) were non-toxic, and only one shoreline dryland plot (P10) exhibited moderate toxicity (Table 2; Figure 4(c1,c2)).

3.2. Leaf Chlorophyll Content in Different Plants Based on Red-Edge Position

Figure 5 presents box plots of red-edge position (REP) for the sampled plant types. The Red-edge position (REP; nm) differed across plant functional types. Elephant grass showed REP values between 704 and 727 nm, oil palm between 703 and 724 nm, Awolowo grass between 703 and 717 nm, mango between 704 and 714 nm, and mangrove vegetation between 695 and 704 nm, with elephant grass exhibiting the longest REP wavelengths, indicating higher chlorophyll concentrations and lower stress levels. In contrast, Awolowo grass, mango trees, and mangroves showed shorter REP wavelengths, reflecting lower chlorophyll content and greater physiological stress.

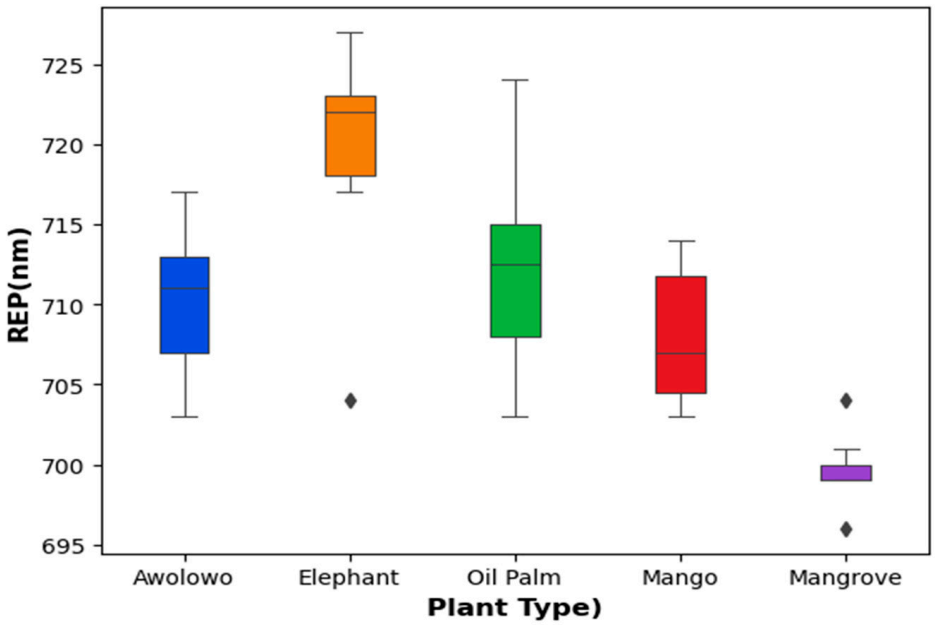

Figure 5. Box plot of REP for different plant types showing outlier with dots.

3.3. Relationship Between Soil Hydrocarbon Parameters and REP

Table 3 presents Pearson and Spearman correlations between REP-derived chlorophyll content and TPH, TOC (%), and EC50 for all vegetation types and individually. Overall, TPHs show no strong or consistent relationship with chlorophyll content across most vegetation types, except for mangroves, which exhibit a moderate negative correlation (r_s = −0.457), indicating reduced chlorophyll with increasing hydrocarbon concentration. In contrast, Awolowo grass and mango trees show positive correlations with TPHs, with mango displaying a moderate Pearson correlation (R = 0.398), suggesting a species-specific response.

Table 3. The correlation between the REP and SHPs.

SHPs	Awolowo Grass		Elephant Grass		Mango Tree		Oil Palm Tree		Mangrove Vegetation		All Plants	
	R	r_s	R	r_s	R	r_s	R	r_s	R	r_s	R	r_s
TPH	0.293	0.242	0.043	0.100	0.398	0.203	−0.199	−0.174	−0.231	−0.457	0.057	−0.061
TOC (%)	0.420	0.456	0.187	0.276	−0.650	−0.657	0.315	0.302	0.324	−0.164	−0.269	−0.208
Soil Toxicity (EC50 mg L^{-1})	−0.094	−0.039	0.27	−0.008	0.401	0.429	−0.180	−0.137	0.007	0.037	0.337	0.355

Note: Red highlight = strong correlation; green highlight = moderate correlation. Correlation coefficients (R and r_s) between 0.1 and 0.3 are considered weak, 0.3–0.5 moderate, and >0.5 strong.

3.4. Relationship Between Soil Hydrocarbon Parameters and HVIs

Table 4 summarises the correlations between SHPs and hyperspectral vegetation indices (HVIs) for each plant type. Overall, TPHs show generally weak relationships with spectral indices across vegetation types, except for mangroves, which display strong negative correlations with mND705 ($R = -0.683$) and PRI ($r_s = -0.667$), indicating reduced chlorophyll performance with increasing hydrocarbon concentration. TOC (%) exhibits contrasting species-specific responses, with Awolowo grass showing positive correlations with chlorophyll-related indices (mND705 $r_s = 0.522$; NDVI $r_s = 0.621$), while mango trees show strong negative correlations (mND705 $R = -0.725$; NDVI $R = -0.564$). EC50 demonstrates the strongest associations overall, particularly for mango (mND705 $r_s = 0.600$; MDATT $r_s = -0.657$) and mangroves (MDATT $R = -0.870$), indicating higher sensitivity of woody vegetation to soil toxicity than to TPH or TOC alone.

Table 4. Correlation between SHPs and HVIs.

	Plant Types	mND 705		PRI		$NDVVI_{844,447}$		MDATT Index	
		R	r_s	R	r_s	R	r_s	R	r_s
(A)	TPH								
	All plants	−0.075	−0.153	−0.250	−0.205	0.071	0.022	0.091	0.106
	Awolowo	0.007	0.025	−0.135	−0.003	0.174	0.179	0.034	−0.091
	Elephant	−0.070	−0.311	0.106	−0.124	0.247	0.173	0.042	0.190
	Mango	0.312	0.058	0.265	0.232	0.143	0.058	−0.582	−0.116
	Palm tree	−0.209	−0.095	−0.323	−0.438	−0.147	−0.105	0.051	0.046
	Mangrove	−0.683	−0.500	−0.351	−0.667	0.368	−0.476	0.275	0.524
(B)	TOC (%)								
	All plants	−0.585	−0.227	−0.537	−0.459	−0.031	−0.027	0.510	0.170
	Awolowo	0.374	0.522	−0.017	0.016	0.486	0.621	−0.279	−0.500
	Elephant	−0.018	−0.011	−0.158	−0.225	0.032	0.110	−0.164	−0.286
	Mango	−0.725	−0.543	−0.339	−0.029	−0.564	−0.371	0.437	0.371
	Palm tree	0.218	0.273	−0.324	−0.413	0.289	0.315	−0.359	−0.483
	Mangrove	−0.276	−0.357	−0.240	−0.119	−0.252	−0.095	0.654	0.405
(C)	Soil toxicity (EC50 mg L^{-1})								
	All plants	0.418	0.379	0.198	0.214	−0.099	0.182	−0.379	−0.363
	Awolowo	0.254	0.104	0.138	−0.115	0.107	−0.198	−0.301	−0.104
	Elephant	0.233	0.137	−0.240	−0.093	−0.344	−0.280	−0.217	−0.126
	Mango	0.416	0.600	−0.343	−0.314	0.335	0.543	−0.264	−0.657
	Palm tree	−0.225	−0.336	−0.331	−0.098	−0.323	−0.371	0.200	0.210
	Mangrove	0.563	0.333	0.531	−0.024	0.627	0.190	−0.870	−0.381

Note: Red highlight = strong correlation; green highlight = moderate correlation. Correlation coefficients (R and r_s) between 0.1 and 0.3 are considered weak, 0.3–0.5 moderate, and >0.5 strong.

4. Discussion

Field spectroscopy is particularly important in the Niger Delta context because vegetation stress induced by hydrocarbon contamination often manifests as subtle changes in leaf pigment composition and physiological function rather than overt canopy loss. Hyperspectral field measurements allow these fine-scale spectral responses—such as shifts in red-edge position and chlorophyll-sensitive indices—to be captured with high precision. These measurements are necessary to interpret EO-derived reflectance signals accurately and to distinguish oil-induced stress from other environmental factors such as nutrient limitation, seasonal variation, or water stress. In this study, we combined the use of field spectroscopy and soil geochemical analysis to afford the leaf-scale characterisation of dominant vegetation responses to hydrocarbon contamination across different plant species and environmental settings in the Niger Delta. Field-derived HVIs are effective tools for detecting vegetation stress associated with hydrocarbon contamination [52]. HVIs derived

from field-based measurements were used to detect the impact of the SHPs on common plant species in the Niger Delta.

4.1. SHP Concentrations Across Land-Cover Types

The concentration of SHPs in the Niger Delta demonstrates a clear spatial heterogeneity in soil hydrocarbon pollution (SHP), reflecting differences among the land-cover types investigated. Overall, TPH concentrations in both dryland and mangrove environments were below the Nigerian Environmental Guidelines and Standards for the Petroleum Industry (EGASPIN) intervention threshold of 5000 mg kg^{-1}, with the notable exception of plot P20 in the mangrove zone, which exceeded the intervention value by approximately 37,000 mg kg^{-1}. Comparable patterns have been reported in previous studies in the Niger Delta, where TPH concentrations were often observed below intervention thresholds [53], although both sub-threshold and exceedance conditions have been documented depending on site-specific factors [54,55]. Variability among studies is likely attributable to differences in spill history, hydrology, and sediment characteristics.

Total organic carbon (TOC) concentrations were markedly higher in mangrove soils than in dryland soils. The average TOC across all samples was 6.10 wt%, with mangrove soils averaging 12.9 wt% and dryland soils averaging 1.40 wt%. TOC values ranged 0.61–26.17 wt% in mangrove soils and 0.50–2.21 wt% in dryland soils. This exceeds the minimum threshold of 0.5 wt% required for hydrocarbon generation in the Niger Delta [56,57]. All mangrove sites exceeded this threshold, whereas only one dryland site (P8) reached the minimum value. The exceptionally high TOC observed in mangrove soils is consistent with global findings that mangroves store substantially more organic carbon than most tropical forest systems due to the accumulation of deep, organic-rich sediments [58]. Comparable high TOC concentrations have been reported along the West African continental margin [59]. Based on established TOC classifications—poor (<0.5%), fair (0.5–1.0%), good (1.0–2.0%), and excellent (>2.0%) [58]—the mangrove soils in this study are categorised as excellent, while the dryland soils are classified as good. The TOC levels reported here are comparable to or exceed those documented in previous studies in the Niger Delta and other tropical coastal environments [56,58,60,61].

The observed soil toxicity patterns clearly differentiate mangrove environments from upland and shoreline dryland settings, with mangrove plots exhibiting consistently higher toxicity levels. This finding aligns with previous studies reporting that mangrove ecosystems function as long-term sinks for hydrocarbons due to low hydrodynamic energy, fine-grained sediments, and high organic matter content that favour contaminant retention [62–64]. Similar elevated toxicity in mangrove soils following oil contamination has been documented in the Niger Delta [65] and other tropical regions [66] where tidal processes redistribute and entrap pollutants within mangrove sediments. These contrasting toxicity conditions are expected to influence vegetation health and stress responses, which will be reflected in the observed variations in chlorophyll content and spectral indices across vegetation types.

4.2. Red-Edge Position Analysis

The mangrove vegetation exhibited the lowest chlorophyll content levels among all the plant types, with the REP between 695 and 704 nm. This pattern is widely associated with reduced chlorophyll content under chronic environmental stress, particularly in hydrocarbon-contaminated, anoxic coastal sediments, where oxygen limitation and pollutant persistence disrupt nutrient uptake and pigment biosynthesis. Long-term exposure to petroleum hydrocarbons impairs photosynthetic efficiency and chloroplast structure in mangroves, leading to sustained physiological degradation even when canopy structure

remains partially intact [67]. Hyperspectral studies show that this degradation is expressed as blue-shifted red-edge responses linked to chlorophyll loss and cellular damage [68]. Zhang et al. [69] reported that field-based and proximal hyperspectral studies of mangrove vegetation demonstrate that degraded or stressed mangroves exhibit a blue shift in the red-edge position toward shorter wavelengths (≈700–710 nm) as a result of chlorophyll degradation and physiological stress. Their results are consistent with our findings; for example, they observed that stressed mangrove vegetation exhibited a peak REP of approximately 703 nm, compared with non-stressed mangrove leaves in a mangrove system in the Mexican Pacific. Similarly, Kuta et al. [3] showed that mangroves exhibited the lowest NDVI values among different vegetation types exposed to hydrocarbons in the Niger Delta.

However, the moderate chlorophyll content exhibited by mango and Awolowo grass may be attributed to their ability to tolerate some levels of hydrocarbon contamination. For instance, ecophysiological studies have shown that *Chromolaena odorata* exhibits relatively high total chlorophyll (Chl a + b) concentrations, particularly under shaded or nutrient-rich conditions [70]. Similarly, the high chlorophyll levels observed in elephant grass and oil palm may be related to their capacity to withstand the impacts of oil spills. Productive grasslands, such as elephant grass, typically exhibit high chlorophyll concentration and rapid biomass turnover [71]. However, studies have shown a significant reduction in the chlorophyll content in fresh palm leaf samples collected from the polluted areas in the Niger Delta [72]. Across these plant functional types, red-edge indices consistently emerge as sensitive indicators of vegetation condition and soil-driven stress, supporting their application in coastal monitoring and remediation assessment.

4.3. Impact of Soil Hydrocarbon Parameters on Plant Types Based on Red-Edge Position (REP)

The relationships between soil hydrocarbon parameters (SHPs) and the red-edge position (REP) reveal clear, species-specific responses, underscoring the sensitivity of the REP as an indicator of vegetation stress and chlorophyll dynamics under contaminated conditions. The REP, which is closely linked to chlorophyll concentration and photosynthetic capacity, responded differently across plant types depending on the dominant soil stressor. Physical changes in plants, expressed through spectra and their derivatives, can be related to oil pollution and other environmental stresses [58]. The general weak REP responses to total petroleum hydrocarbons (TPHs) across vegetation types indicate that TPHs alone do not consistently drive spectral shifts in chlorophyll. The moderate negative correlations observed for mangrove vegetation may indicate reduced chlorophyll content, as observed in the previous section, and stress-induced REP shifts under increasing hydrocarbon concentrations. The mangrove has been recognised as highly vulnerable to oil spills [64,73]. The negligible relationship observed when all vegetation types were pooled highlights the strong moderating role of species traits.

In contrast, TOC (%) exerted more differentiated effects on the REP. Moderate positive correlations for Awolowo and oil palm suggest that soil organic carbon supports chlorophyll maintenance for these species. Conversely, we observed a negative correlation between mango leaf chlorophyll and soil total organic carbon (TOC), which likely reflects the dominance of petroleum-derived and recalcitrant organic matter rather than biologically available carbon. However, the lack of impact of toxicity on the mangrove vegetation may be due to the consistent chronic contaminant accumulation. However, the influence of soil toxicity on the REP, particularly for mango trees, could indicate high sensitivity and chlorophyll suppression under toxic conditions. Overall, the findings demonstrate that the REP effectively captures vegetation stress responses to soil hydrocarbon parameters while also emphasising the need for species-specific interpretation in oil-impacted environments. The discussion on the impact of SHPs on plant types will buttress these findings.

4.4. Impact of Soil Hydrocarbon Parameters on Plant Types

Vegetation responses to total petroleum hydrocarbons (TPHs) were consistent with stress patterns previously identified using red-edge-based assessments. Mangrove vegetation exhibited the strongest adverse response, reinforcing its well-documented sensitivity to oil contamination due to sediment-trapping and prolonged pollutant retention [64]. Similar degradation of mangroves following oil spills has been widely reported in remote sensing studies in the Niger Delta [3,10]. Oil palm and elephant grass also showed moderate signs of stress. For oil palm, it indicates reduced photosynthetic efficiency consistent with hydrocarbon-induced physiological stress previously observed in field spectrometer studies by Jamaludin et al. [74]. However, for elephant grass, previous studies have shown that elephant grass (*Pennisetum purpureum*) exposed to hydrocarbon-contaminated conditions, particularly at moderate to high contamination levels, maintains growth, which can be effectively used as a low-cost and environmentally sustainable solution for remediating petroleum-contaminated soil [75,76]. However, the studies were done under controlled conditions and were not remote sensing-based.

In contrast, while mango trees exhibited positive sensitivity to TPHs, Awolowo grass was insensitive, consistent with previous findings from the REP, which could highlight their tolerance and adaptive persistence in hydrocarbon-contaminated soils. Studies have shown that mango leaves and bark have been used for the removal of TPHs from soil [77]. Similarly, Awolowo grass (commonly identified as carpet grass, *Axonopus compressus*) is widely reported to be relatively tolerant to hydrocarbon contamination in oil-impacted soil. Awolowo grass has been shown to tolerate oil contamination in soil [78] and reduce the concentration of heavy metals in polluted soils [79]. The sunflower family (to which Awolowo grass belongs) can survive soil hydrocarbon contamination of approximately 18,000 mg/kg by metabolic changes in chlorophyll a, total chlorophyll and carotenoids, showing no significant decrease under these conditions [80].

Vegetation responses to soil organic carbon (TOC) showed clear species-specific patterns consistent with earlier red-edge position (REP) behaviour. Elevated TOC was generally associated with increased physiological stress rather than improved plant condition, indicating that organic carbon in oil-impacted soils likely reflects contamination-derived inputs rather than bioavailable fertility [81]. This is supported by REP evidence of chlorophyll suppression at high TOC levels. Mango and mangrove vegetation exhibited the strongest sensitivity, reinforcing their vulnerability to contaminated organic matter accumulation. In contrast, Awolowo grass showed a more favourable response, consistent with chlorophyll stability and tolerance reported in earlier REP analysis. Elephant grass and oil palm displayed weaker or mixed responses, suggesting limited benefit from elevated TOC under contaminated conditions.

Vegetation responses to soil toxicity, expressed through EC50, reveal species-specific sensitivity patterns that align with earlier REP-based stress indicators. Mangrove vegetation exhibited the strongest sensitivity to toxic conditions, indicating severe physiological impairment under elevated soil toxicity, consistent with REP shifts linked to chlorophyll degradation and sustained stress. Mango trees showed high sensitivity, reinforcing REP evidence of reduced photosynthetic functioning under toxic exposure. In contrast, Awolowo and elephant grasses displayed weaker responses, suggesting greater tolerance to toxic soils and limited physiological disruption, consistent with grass resilience reported in contaminated environments. Similarly, oil palm was not impacted by toxicity, indicating reduced resilience relative to grasses. Overall, the agreement between EC50-derived responses and REP patterns confirms soil toxicity as a driver of vegetation stress. However, there are a lack of studies on the relationship of TOC (%) of plant types exposed to oil spill for comparative analysis.

5. Conclusions

This study developed an integrated earth observation (EO) and geochemical framework to assess vegetation stress associated with soil hydrocarbon contamination in the Niger Delta, a highly impacted coastal and deltaic system. Using field measurements of total petroleum hydrocarbons, soil toxicity (EC50), and total organic carbon alongside leaf-scale hyperspectral analysis and red-edge position (REP), the present research study identified clear species-specific responses to contamination. Mangrove and oil palm tree showed the greatest sensitivity to hydrocarbon stress, while Mango and mangrove showed the strongest sensitivity to soil toxicity, and Awolowo grass consistently exhibited tolerance across contamination gradients. Methodologically, this study demonstrates the value of hyperspectral and red-edge-based approaches for linking vegetation stress to underlying soil pollution in complex coastal landscapes. However, the analysis is limited by its single-period design, the absence of an uncontaminated control site, and the integrative nature of the REP, which reflects combined stressors rather than individual contamination pathways.

Future work should incorporate control sites, multi-temporal EO observations, and higher-resolution UAV hyperspectral data to strengthen causal interpretation and support long-term coastal pollution monitoring and management.

Author Contributions: Conceptualisation, A.A.K.; Methodology, A.A.K., S.G., D.S.B. and C.H.V.; Software, A.A.K.; Validation, A.A.K., S.G. and D.S.B.; Formal Analysis, A.A.K.; Investigation, A.A.K.; Resources, A.A.K., S.G. and D.S.B.; Data Curation, A.A.K.; Writing—Original Draft Preparation, A.A.K.; Writing—Review and Editing, A.A.K., S.G., D.S.B. and C.H.V.; Visualisation, A.A.K.; Supervision, S.G. and D.S.B.; Project Administration, A.A.K.; Funding Acquisition, A.A.K. All authors have read and agreed to the published version of the manuscript.

Funding: This research study was funded by the Petroleum Technology Development Fund (PTDF) under the Federal Government of Nigeria (PTDF/ED/PHD/KAA/966/16).

Data Availability Statement: The original contributions presented in this study are included in the article. Further inquiries can be directed to the corresponding author.

Acknowledgments: The authors wish to express their sincere gratitude to Bolaji Babatunde from the Department of Animal and Environmental Biology, Faculty of Science, for organising the fieldwork and to Goodluck Nwipie Nakaima from the Department of Fisheries, University of Port Harcourt, for coordinating logistics and contributing as a member of the field team during data collection.

Conflicts of Interest: Author Stephen Grebby was employed by the company UK Terra Motion Limited. The remaining authors declare that the research was conducted in the absence of any commercial or financial relationships that could be construed as a potential conflict of interest.

References

1. Okoye, C.O.; Okunrobo, L.A. Impact of Oil Spill on Land and Water and Its Health Implications in Odu- Gboro Community, Sagamu, Ogun State, Nigeria. *World J. Environ. Sci. Eng.* **2014**, *1*, 1–211.
2. Umar, A.T.; Hajj Othman, M.S. Causes and Consequences of Crude Oil Pipeline Vandalism in the Niger Delta Region of Nigeria: A Confirmatory Factor Analysis Approach. *Cogent Econ. Financ.* **2017**, *5*, 1353199. [CrossRef]
3. Kuta, A.A.; Grebby, S.; Boyd, D.S. Remote Monitoring of the Impact of Oil Spills on Vegetation in the Niger Delta, Nigeria. *Appl. Sci.* **2025**, *15*, 338. [CrossRef]
4. Anejionu, O.C.D.; Ahiarammunnah, P.A.N.; Nri-ezedi, C.J. Hydrocarbon Pollution in the Niger Delta: Geographies of Impacts and Appraisal of Lapses in Extant Legal Framework. *Resour. Policy* **2015**, *45*, 65–77. [CrossRef]
5. Osuagwu, A.N.; Okigbo, A.U.; Ekpo, I.A.; Chukwurah, P.N.; Agbor, R.B.; Bessong Agbor, R. Effect of Crude Oil Pollution on Growth Parameters, Chlorophyll Content and Bulbils Yield in Air Potato (*Dioscorea bulbifera* L.). *Int. J. Appl. Sci. Technol.* **2013**, *3*, 37–42.
6. Adamu, B.; Tansey, K.; Ogutu, B. Using Vegetation Spectral Indices to Detect Oil Pollution in the Niger Delta. *Remote Sens. Lett.* **2015**, *6*, 145–154. [CrossRef]

7. Piro, P.; Porti, M.; Veltri, S.; Lupo, E.; Moroni, M. Hyperspectral Monitoring of Green Roof Vegetation Health State in Sub-Mediterranean Climate: Preliminary Results. *Sensors* **2017**, *17*, 662. [CrossRef]
8. Onyia, N.N.; Balzter, H.; Berrio, J.C. Normalized Difference Vegetation Vigour Index: A New Remote Sensing Approach to Biodiversity Monitoring in Oil Polluted Regions. *Remote Sens.* **2018**, *10*, 897.
9. Omodanisi, E.O.; Salami, A.T. An Assessment of the Spectra Characteristics of Vegetation in South Western Nigeria. *IERI Procedia* **2014**, *9*, 26–32. [CrossRef]
10. Adamu, B.; Tansey, K.; Ogutu, B. Remote Sensing for Detection and Monitoring of Vegetation Affected by Oil Spills. *Int. J. Remote Sens.* **2018**, *39*, 3628–3645. [CrossRef]
11. Adebangbe, S.A.; Dixon, D.P.; Barrett, B. Evaluating Contaminated Land and the Environmental Impact of Oil Spills in the Niger Delta Region: A Remote Sensing-Based Approach. *Environ. Monit. Assess.* **2025**, *197*, 1149. [CrossRef]
12. Ozigis, M.S.; Kaduk, J.D.; Jarvis, C.H.; da Conceição Bispo, P.; Balzter, H. Detection of Oil Pollution Impacts on Vegetation Using Multifrequency SAR, Multispectral Images with Fuzzy Forest and Random Forest Methods. *Environ. Pollut.* **2019**, *256*, 113360. [CrossRef]
13. O'Farrell, J.; O'Fionnagáin, D.; Babatunde, A.O.; Geever, M.; Codyre, P.; Murphy, P.C.; Spillane, C.; Golden, A. Quantifying the Impact of Crude Oil Spills on the Mangrove Ecosystem in the Niger Delta Using AI and Earth Observation. *Remote Sens.* **2025**, *17*, 358. [CrossRef]
14. Ozigis, M.S.; Kaduk, J.D.; Jarvis, C.H. Mapping Terrestrial Oil Spill Impact Using Machine Learning Random Forest and Landsat 8 OLI Imagery: A Case Site within the Niger Delta Region of Nigeria. *Environ. Sci. Pollut. Res.* **2019**, *26*, 3621–3635. [CrossRef]
15. Adamu, B. Broadband Multispectral Indices for Remote Sensing of Vegetation Affected by Oil Spills in the Mangrove Forest of the Niger Delta, Nigeria. Ph.D. Thesis, University of Leicester, Leicester, UK, 2016.
16. Gunderson, J. The Effect of Hydrocarbon Contamination and Mycorrhizal Inoculation on Poplar Fine Root Dynamics. Master's Thesis, University of Saskatchewan, Saskatchewan, SK, Canada, 2006. Available online: https://harvest.usask.ca/items/e73ec50e-9177-4880-a153-e1416d49aad3 (accessed on 12 January 2022).
17. Pegg, S.; Zabbey, N. Oil and Water: The Bodo Spills and the Destruction of Traditional Livelihood Structures in the Niger Delta. *Community Dev. J.* **2013**, *48*, 391–405. [CrossRef]
18. Koutika, L.S.; Rainey, H.J. Chromolaena Odorata in Different Ecosystems: Weed or Fallow Plant? *Appl. Ecol. Environ. Res.* **2010**, *8*, 131–142. [CrossRef]
19. Uyi, O.O.; Ekhator, F.; Ikuenobe, C.E.; Borokini, T.I.; Aigbokhan, E.I.; Egbon, I.N.; Adebayo, A.R.; Igbinosa, I.B.; Okeke, C.O.; Igbinosa, E.O.; et al. Chromolaena Odorata Invasion in Nigeria: A Case for Coordinated Biological Control. *Manag. Biol. Invasions* **2014**, *5*, 377–393. [CrossRef]
20. Taiwo, O.B.; Olajide, O.A.; Soyannwo, O.O.; Makinde, J.M. Anti-Inflammatory, Antipyretic and Antispasmodic: Properties of Chromolaena Odorata. *Pharm. Biol.* **2000**, *38*, 367–370. [CrossRef]
21. Singh, B.P.; Singh, H.P.; Obeng, E. Elephantgrass. In *Biofuel Crops: Production, Physiology and Genetics*; CABI: Wallingford, UK, 2015.
22. Dessalegn, Y.; Assefa, H.; Derso, T.; Tefera, M. Mango Production Knowledge and Technological Gaps of Smallholder Farmers in Amhara Region, Ethiopia. *Am. Sci. Res. J. Eng. Technol. Sci.* **2014**, *10*, 28–39.
23. Kumar, M.; Saurabh, V.; Tomar, M.; Hasan, M.; Changan, S.; Sasi, M.; Maheshwari, C.; Prajapati, U.; Singh, S.; Prajapat, R.K.; et al. Mango (*Mangifera indica* L.) Leaves: Nutritional Composition, Phytochemical Profile, and Health-Promoting Bioactivities. *Antioxidants* **2021**, *10*, 299. [CrossRef]
24. Bally, I.S.E. Mangifera Indica (Mango). In *Species Profiles for Pacific Island Agroforestry*; Version 3.1; 2006; Volume 25. Available online: https://agroforestry.org/ (accessed on 5 May 2026).
25. Barcelos, E.; De Almeida Rios, S.; Cunha, R.N.V.; Lopes, R.; Motoike, S.Y.; Babiychuk, E.; Skirycz, A.; Kushnir, S. Oil Palm Natural Diversity and the Potential for Yield Improvement. *Front. Plant Sci.* **2015**, *6*, 190. [CrossRef]
26. Aghalino, S.O. British Colonial Policies and the Oil Palm Industry in the Niger Delta Region of Nigeria, 1900–1960. *Afr. Study Monogr.* **2000**, *21*, 19–33.
27. Punnuri, S.M.; Singh, B.P. Oil Palm. In *Biofuel Crops: Production, Physiology and Genetics*; CABI: Wallingford, UK, 2013; pp. 392–414.
28. Ayanlade, A. Remote Sensing of Environmental Change in the Niger Delta. Ph.D. Thesis, University of London, London, UK, 2014.
29. Harcourt, P. Socio Economic Importance of Red Mangrove (*Rhizophora racemosa* L.) to Rural Dwellers in Southern Nigeria. *J. Nat. Sci. Res.* **2012**, *2*, 182–186.
30. Kuta, A.A. Characterising Land Cover Changes in the Niger Delta Caused by Oil Production. Ph.D. Thesis, University of Nottingham, Nottingham, UK, 2023. Available online: https://nusearch.nottingham.ac.uk/discovery/fulldisplay/alma9922779354905561/44NOTTS_UNUK:44NOTUK (accessed on 24 January 2024).
31. Arellano, P.; Tansey, K.; Balzter, H.; Tellkamp, M. Plant Family-Specific Impacts of Petroleum Pollution on Biodiversity and Leaf Chlorophyll Content in the Amazon Rainforest of Ecuador. *PLoS ONE* **2017**, *12*, e0169867. [CrossRef] [PubMed]

32. Arellano, P.; Tansey, K.; Balzter, H.; Boyd, D.S. Detecting the Effects of Hydrocarbon Pollution in the Amazon Forest Using Hyperspectral Satellite Images. *Environ. Pollut.* **2015**, *205*, 225–239. [CrossRef] [PubMed]
33. Abdullah, H.; Darvishzadeh, R.; Skidmore, A.K.; Groen, T.A.; Heurich, M. European Spruce Bark Beetle (*Ips typographus* L.) Green Attack Affects Foliar Reflectance and Biochemical Properties. *Int. J. Appl. Earth Obs. Geoinf.* **2018**, *64*, 199–209. [CrossRef]
34. NREC. NERC Field Spectroscopy Facility ASD FieldSpec Pro System. Available online: https://fsf.nerc.ac.uk/ (accessed on 1 September 2018).
35. Martinez, N.E.; Sharp, J.L.; Johnson, T.E.; Kuhne, W.W.; Stafford, C.T.; Duff, M.C. Reflectance-Based Vegetation Index Assessment of Four Plant Species Exposed to Lithium Chloride. *Sensors* **2018**, *18*, 2750. [CrossRef]
36. Walker, P. *Guidlines fo Post Processing ASD FieldSpec Pro andFieldSpec 3 Spectral Data Files Using the FSF MS Excel Template*; NERC Field Spectroscopy Facility: Edinburg, UK, 2009.
37. Serrano-Calvo, R.; Cutler, M.E.J.; Bengough, A.G. Spectral and Growth Characteristics of Willows and Maize in Soil Contaminated with a Layer of Crude or Refined Oil. *Remote Sens.* **2021**, *13*, 3376. [CrossRef]
38. Vane, C.H.; Kim, A.W.; Moss-Hayes, V.; Turner, G.; Mills, K.; Chenery, S.R.; Barlow, T.S.; Kemp, A.C.; Engelhart, S.E.; Hill, T.D.; et al. Organic Pollutants, Heavy Metals and Toxicity in Oil Spill Impacted Salt Marsh Sediment Cores, Staten Island, New York City, USA. *Mar. Pollut. Bull.* **2020**, *151*, 110721. [CrossRef] [PubMed]
39. Vane, C.H.; Turner, G.H.; Chenery, S.R.; Richardson, M.; Cave, M.C.; Terrington, R.; Gowing, C.J.B.; Moss-Hayes, V. Trends in Heavy Metals, Polychlorinated Biphenyls and Toxicity from Sediment Cores of the Inner River Thames Estuary, London, UK. *Environ. Sci. Process. Impacts* **2020**, *22*, 364–380. [CrossRef]
40. Ramage, C.I.; Lopes dos Santos, R.A.; Yon, L.; Johnson, M.F.; Vane, C.H. Widespread Pesticide Pollution in Two English River Catchments of Contrasting Land-Use: From Sediments to Fish. *Environ. Pollut.* **2025**, *375*, 126371. [CrossRef]
41. Vane, C.H.; Harrison, I.; Kim, A.W. Polycyclic Aromatic Hydrocarbons (PAHs) and Polychlorinated Biphenyls (PCBs) in Sediments from the Mersey Estuary, UK. *Sci. Total Environ.* **2007**, *374*, 112–126. [CrossRef]
42. Blackburn, G.A. Spectral Indices for Estimating Photosynthetic Pigment Concentrations: A Test Using Senescent Tree Leaves. *Int. J. Remote Sens.* **1998**, *19*, 657–675. [CrossRef]
43. Filella, I.; Peñuelas, J. The Red Edge Position and Shape as Indicators of Plant Chlorophyll Content, Biomass and Hydric Status. *Int. J. Remote Sens.* **1994**, *15*, 1459–1470. [CrossRef]
44. Mutanga, O.; Skidmore, A.K. Red Edge Shift and Biochemical Content in Grass Canopies. *ISPRS J. Photogramm. Remote Sens.* **2007**, *62*, 34–42. [CrossRef]
45. Sims, D.A.; Gamon, J.A. Relationships between Leaf Pigment Content and Spectral Reflectance across a Wide Range of Species, Leaf Structures and Developmental Stages. *Remote Sens. Environ.* **2002**, *81*, 337–354. [CrossRef]
46. Velichkova, K.; Krezhova, D. Comparative Analysis of Hyperspectral Vegetation Indices for Remote Estimation of Leaf Chlorophyll Content and Plant Status. *RAD. Assoc. J.* **2019**, *3*, 202–208. [CrossRef]
47. Lu, S.; Lu, X.; Zhao, W.; Liu, Y.; Wang, Z.; Omasa, K. Comparing Vegetation Indices for Remote Chlorophyll Measurement of White Poplar and Chinese Elm Leaves with Different Adaxial and Abaxial Surfaces. *J. Exp. Bot.* **2015**, *66*, 5625–5637. [CrossRef] [PubMed]
48. Gamon, J.A.; Serrano, L.; Surfus, J.S. The Photochemical Reflectance Index: An Optical Indicator of Photosynthetic Radiation Use Efficiency across Species, Functional Types, and Nutrient Levels. *Oecologia* **1997**, *112*, 492–501. [CrossRef]
49. Gitelson, A.; Merzlyak, M.N. Quantitative Estimation of Chlorophyll-a Using Reflectance Spectra: Experiments with Autumn Chestnut and Maple Leaves. *J. Photochem. Photobiol. B* **1994**, *22*, 247–252. [CrossRef]
50. Statisticssolutions.com Pearson's Correlation Coefficient. Available online: https://www.statisticssolutions.com/free-resources/directory-of-statistical-analyses/pearsons-correlation-coefficient/ (accessed on 11 September 2021).
51. Schober, P.; Schwarte, L.A. Correlation Coefficients: Appropriate Use and Interpretation. *Anesth. Analg.* **2018**, *126*, 1763–1768. [CrossRef] [PubMed]
52. Measuring Total Organic Carbon in Soil. Available online: https://spectralevolution.s3.us-east-2.amazonaws.com/assets/20171103190638/TOC_App_Note.pdf (accessed on 24 March 2026).
53. Alinnor, I.J.; Nwachukwu, M.A. Determination of Total Petroleum Hydrocarbon in Soil and Groundwater Samples in Some Communities in Some Communities in River State, Nigeria. *J. Environ. Chem. Ecotoxicol.* **2013**, *5*, 292–297. [CrossRef]
54. Little, D.I.; Holtzmann, K.; Gundlach, E.R.; Galperin, Y. Sediment Hydrocarbons in Former Mangrove Areas, Southern Ogoniland, Eastern Niger Delta, Nigeria. *Coast. Res. Libr.* **2018**, *25*, 323–342. [CrossRef]
55. UNEP. *Environmental Assessment of Ogoniland*; UNEP: Nairobi, Kenya, 2011; ISBN 9789280731309.
56. Fadiya, S.L.; Adekola, S.A.; Oyebamiji, B.M.; Akinsanpe, O.T. Source Rock Geochemistry of Shale Samples from Ege-1 and Ege-2 Wells, Niger Delta, Nigeria. *J. Pet. Explor. Prod. Technol.* **2020**, *11*, 579–586. [CrossRef]
57. Oyonga, O.A.; Itam, A.E.; Etete, E.N. Petrophysical Evaluation of Total Organic Carbon Content (TOC) in Gbada Formation, Niger Delta Basin. *GSJ* **2018**, *6*, 324–329.

58. Onyena, A.P.; Sam, K. A Review of the Threat of Oil Exploitation to Mangrove Ecosystem: Insights from Niger Delta, Nigeria. *Glob. Ecol. Conserv.* **2020**, *22*, e00961. [CrossRef]
59. Seiter, K.; Hensen, C.; Schröter, J.; Zabel, M. Organic Carbon Content in Surface Sediments-Defining Regional Provinces. *Deep. Sea. Res. Part I Oceanogr. Res. Pap.* **2004**, *51*, 2001–2026. [CrossRef]
60. Umar, H.A.; Abdul Khanan, M.F.; Ogbonnaya, C.; Shiru, M.S.; Ahmad, A.; Baba, A.I. Environmental and Socioeconomic Impacts of Pipeline Transport Interdiction in Niger Delta, Nigeria. *Heliyon* **2021**, *7*, e06999. [CrossRef]
61. Falebita, D.E.; Ayeni, O.Z.; Bayowa, O.G.; Anukwu, G.C. Study of the Organic Richness and Petrophysical Characteristics of Selected Shales from the Analysis of Wireline Logs: A Case of "Neya" Field, Niger Delta. *Ife J. Sci.* **2015**, *17*, 41–52.
62. TRCC. *Niger Delta Mangrove Citizen Science Project*; Tropical Research and Conservation Centre (TRCC): Uyo, Nigeria. Available online: https://www.oneplanetnetwork.org/sites/default/files/niger_delta_mangrove_citizen_science_project.pdf (accessed on 3 March 2021).
63. Alongi, D.M. Present State and Future of the World's Mangrove Forests. *Environ. Conserv.* **2002**, *29*, 331–349. [CrossRef]
64. Duke, N.C. Oil Spill Impacts on Mangroves: Recommendations for Operational Planning and Action Based on a Global Review. *Mar. Pollut. Bull.* **2016**, *109*, 700–715. [CrossRef]
65. Chris, D.I.; Anyanwu, B.O. Pollution and Potential Ecological Risk Evaluation Associated with Toxic Metals in an Impacted Mangrove Swamp in Niger Delta, Nigeria. *Toxics* **2023**, *11*, 6. [CrossRef] [PubMed]
66. Wu, G.R.; Hong, H.L.; Yan, C.L. Arsenic Accumulation and Translocation in Mangrove (*Aegiceras corniculatum* L.) Grown in Arsenic Contaminated Soils. *Int. J. Environ. Res. Public Health* **2015**, *12*, 7244–7253. [CrossRef]
67. Naidoo, G. Oil Pollution in Mangroves: A Review. *Forests* **2025**, *17*, 43. [CrossRef]
68. Hoque, E.; Hutzler, P.J.S. Spectral Blue-Shift of Red Edge Minitors Damage Class of Beech Trees. *Remote Sens. Environ.* **1992**, *39*, 81–84. [CrossRef]
69. Zhang, C.; Kovacs, J.M.; Wachowiak, M.P.; Flores-Verdugo, F. Relationship between Hyperspectral Measurements and Mangrove Leaf Nitrogen Concentrations. *Remote Sens.* **2013**, *5*, 891–908. [CrossRef]
70. Naidoo, K.K. Ecophysiological Studies of the Invasive Weed *Chromolaena odorata* (L.) King and Robinson and Its Control in KwaZulu-Natal. Ph.D. Thesis, University of KwaZulu-Natal, Durban, South Africa, 2013.
71. Magalhães Bueno, A.; De Andrade, A.F.; Viçosi, K.A.; Flores, A.R.; Sette, C.R.; Da Cunha, T.Q.G. Does Nitrogen Application Improve Elephant Grass Yield and Energetic Characteristics of Biofuels? *BioEnergy Res.* **2021**, *14*, 774–784. [CrossRef]
72. Otitoju, O.; Onwurah, I.N.E. Chlorophyll Contents of Oil Palm (*Elaeis guineensis*) Leaves Harvested from Crude Oil Polluted Soil: A Shift in Productivity Dynamic. *Sch. Res. Libr. Ann. Biol. Res.* **2010**, *1*, 20–27.
73. Hoff, R.; Hensel, P.; Yender, R.; Mearns, A.J.; Michel, J.; Proffitt, E.C.; Shigenaka, G.; Hoff, R.; Michel, J.; Michel, J.; et al. Oil Spills in Mangroves: Planning & Response Considerations. 2014. Available online: https://repository.library.noaa.gov/view/noaa/877 (accessed on 11 February 2022).
74. Jamaludin, M.I.; Matori, A.N.; Myint, K.C. Application of NIR to Determine Effects of Hydrocarbon Microseepage in Oil Palm Vegetation Stress. In Proceedings of the 2015 International Conference on Space Science and Communication, Langkawi, Malaysia, 10–12 August 2015.
75. Bobor, L.O.; Omosefe, B.E. Elephant Grass (*Pennisetum purpureum*) Mediated Phytoremediation of Crude Oil-Contaminated Soil. *Niger. J. Environ. Sci. Technol.* **2019**, *3*, 105–111. [CrossRef]
76. Udom, N.R.; Ogwo, P.A.; Uchendu, U.I. Crude Oil Remediation Potentials of *Pennisetum purpureum* in Oil Producing Communities of Akwa Ibom State, Nigeria. *J. Health Appl. Sci. Manag.* **2024**, *7*, 245–254. [CrossRef]
77. Ehirim, O.; Walter, C.; Ukpaka, C. Mix Model Formulation for TPH Prediction during Bioremediation of Hydrocarbon Contaminated Soils. *Am. J. Eng. Res.* **2020**, *9*, 1–11.
78. Ikhajiagbe, B.; Akindolor, A. Comparative Effects of Pretreatment of Stem Cuttings of Chromolaena Odorata (*Siam weed*) with Sodium Azide and Hydroxylamide on the Survival and Phyoremediative Performance in an Oil-Polluted Soil. *Niger. J. Biotechnol.* **2016**, *31*, 27. [CrossRef]
79. Ayesa, S.A.; Chukwuka, K.S.; Odeyemi, O.O. Tolerance of Tithonia Diversifolia and Chromolaena Odorata in Heavy Metal Simulated-Polluted Soils and Three Selected Dumpsites. *Toxicol. Rep.* **2018**, *5*, 1134–1139. [CrossRef]
80. Rahbar, F.G.; Kiarostami, K.; Shirdam, R. Effects of Petroleum Hydrocarbons on Growth, Photosynthetic Pigments and Carbohydrate Levels of Sunflower. *J. Food Agric. Environ.* **2012**, *10*, 773–776.
81. Essien, O.E.; John, I.A. Impact of Crude-Oil Spillage Pollution and Chemical Remediation on Agricultural Soil Properties and Crop Growth. *J. Appl. Sci. Environ. Manag.* **2010**, *14*, 147–154. [CrossRef]